Radio Interferometric Object Tracking

Gergely Zachár, Gyula Simon
Department of Computer Science and Systems Technology
University of Pannonia
Veszprém, Hungary
{zachar, simon}@dcs.uni-pannon.hu

Miklós Maróti
Bolyai Institute
University of Szeged
Szeged, Hungary
mmaroti@math.u-szeged.hu

Abstract—**This paper proposes a novel object tracking method using radio interferometry. The proposed low cost solution is able to track objects, equipped with a radio receiver, in real time, using only simple infrastructure nodes with radio transceivers at fixed and known locations. The localization method has low computational requirements and does not require any preliminary knowledge of, or measurements in the space where tracking is performed. The paper introduces the novel method and preliminary test results are also presented.**

Keywords–radio interferometry; positioning; sensor networks

I. INTRODUCTION

Location-Based Services are important building blocks of several applications, e.g. surveillance, mobiles robots, or various industrial and supply chain tracking applications. To determine the location of objects there exist numerous approaches, e.g. the Global Positioning System (GPS), indoor positioning systems using Wi-Fi RF signals, RFID tags, or systems using images taken by inexpensive cameras.

In this paper a novel tracking mechanism is introduced, which uses fixed transmitter and receiver nodes to track the movement of a receiver node, when its initial position is known. The method uses radio interferometry, where two transmitters generate an interference signal, which can be used to retrieve information regarding the relative positions of the transmitters and two receivers, one being the moving node. With successive measurements the system is able to track the movement of one or multiple objects.

In Section II related work is reviewed. Section III introduces the novel tracking method. Preliminary measurement results are presented in Section IV, to illustrate the capabilities of the proposed method. Section V concludes the paper.

II. PREVIOUS WORK

A. *Object posioning and tracking*

In outdoor positioning nowadays GPS is the most dominant method, with accuracy of a few meters. With special differential methods the accuracy can be decreased below 1m. The operation of GPS receivers requires line of sight of reference satellites, thus the applicability of GPS indoors is very limited. In indoor positioning a large variety of competitive methods have been proposed, using acoustic ranging, image processing, and radio signals, just to name a few.

Methods using acoustic (mainly ultrasound) ranging measure the time of flight of acoustic beacons and compute pairwise distances (ranges). From the measured ranges and the known locations of the beacons the position of the object can be estimated [1].

Low cost image processing in used in [2] for localization, where graphical markers are used (e.g. to identify key positions in a museum). A simple camera phone is used to take a picture on the marker and the localization is performed based on a static digital map. More advanced systems use a large set of pictures taken in the streets or buildings, and the localization is performed by comparing the photograph taken at an unknown position to the stored picture database [3].

Radio signals are widely used in indoor positioning. Signal-strength based measurements utilize several transmitter sources and a map, which indicates the expected received signal strength (RSSI) of the transmitters at various positions of the space. Based on RSSI measurements the actual position of a receiver can be approximated [4].

Time of flight of RF signals is used for ranging in [5]. The pairwise ranges can be used for localization, similarly to other (e.g. acoustic) ranging methods. To increase accuracy of ranging in multipath environments time of flight measurements were combined with phase evaluation in [6]. A completely different RF-based solution was proposed in [7], based on interference of radio signals.

B. *Radio Interferometric Positioning*

Radio Interferometric Positioning [7] was designed to provide low cost localization in wireless sensor networks, utilizing inexpensive off the shelf components. The method does not use high frequency signal processing, instead relies on radio interferometry and processes low frequency interference signals. The method utilizes two transmitters (A and B) to create an interference signal at two receivers (C and D), as shown in Fig. 1. If the frequencies of the two transmitters are approximately the same ($f_A \approx f_B \approx f$) then the interference signal at the receivers will have a low frequency envelope with frequency $\Delta f = |f_A - f_B|$. This low frequency signal is the actual RSSI signal, which is available on most RF transceivers.

By measuring the phase difference ϑ between the RSSI signals detected at two receivers, information on the relative positions of the four nodes involved can be gained as follows [7]:

This work was partially supported by the Hungarian State and the European Union under projects TAMOP-4.2.2.A-11/1/KONV-2012-0073 and TAMOP-4.2.2.-C-11/1/KONV- 2012-0004.

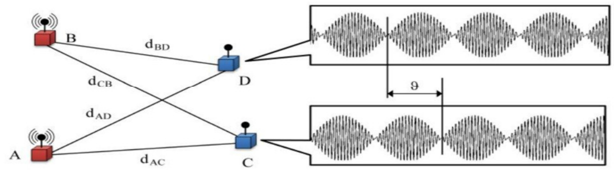

Figure 1. Radio interferometric phase measurement

$$\vartheta(f) = 2\pi \frac{d_{ABCD}}{c/f} \ (mod\ 2\pi) \tag{1}$$

where c is the speed of light and the *quad-range* d_{ABCD} is defined as follows:

$$\mathrm{d_{ABCD}} = \mathrm{d_{AD}} - \mathrm{d_{BD}} + \mathrm{d_{BC}} - \mathrm{d_{AC}} \tag{2}$$

(see Fig. 1 for distance notations). Note that the quad-range is not an ordinary (pairwise) range but rather it provides a linear combination of the pairwise ranges of the four nodes involved. Also note the modulo operator in (1), which results an ambiguity of the solution: exact quad-ranges cannot be determined from one measurement. The phase ambiguity can be resolved by using multiple carrier frequencies and thus multiple $\vartheta(f)$ values. Solving a Diophantine equation the exact value of the quad-range d_{ABCD} can be calculated (see [7]), provided the phase measurements have very small errors. Unfortunately this is rarely true in uncontrolled environments, as will be illustrated in our measurement results (see e.g. Fig. 9).

From the calculated quad-ranges the object location is determined by an optimization method, based on genetic algorithms. The method proposed in [7] requires a large amount of data to be collected (in [7] 80 minutes data collection time was reported, but for smaller scale setups 5 minutes of latency was estimated) and the localization also computationally intensive (2 minutes of calculation for the experiment in [7]).

In the next section a novel method will be proposed to track objects. The proposed method is much less sensitive to measurement uncertainties, and provides fast tracking for objects.

III. Radio Interferometric Tracking

Our proposed method is not a pure localization but rather a tracking technique. We assume that the initial position of the object is known and the movement of the object is tracked in time by successive measurements.

The system uses fixed reference nodes (transmitters and receivers) and arbitrary number of tracked receiver nodes. For sake of simplicity we will discuss only the case of one tracked node. First we will discuss the phase measurement process, then tracking in one dimension will be discussed, finally we will show how to extend tracking to multiple dimensions.

A. Phase difference measurement

The two receivers C and D are synchronized to each other. In the current solution a reference broadcast start command is used both to start measurement and provide time synchronization between the receiver nodes [9]. After the start command each receiver nodes sample the RSSI of the received

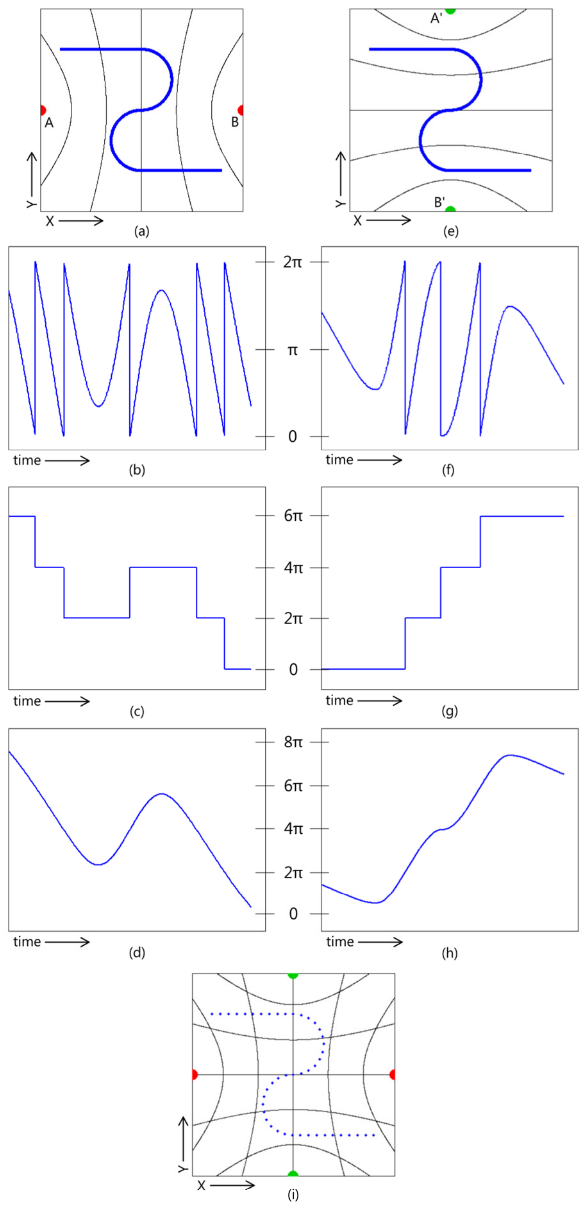

Figure 2. Radio interferometric tracking with fixed transmitters A, B, A', B', fixed receiver C=C', positioned at the center (not shown for clarity), and moving node D. (a) The generated phase pattern by transmitters A and B: hiperbolas corresponding to $\vartheta = 2k\pi$ phase values are shown. The trajectory of the moving object is shown by thick line, the origin is assumed to be known, (b) the measured phase difference values between nodes C and D, (c) phase correction values, (d) unwrapped phase values, (e)-(h) independent measurement with transmitters A' and B', (i) tracking using the phase esimates of the two measurements. The trajectory estimate is shown by the dotted line.

interference signal for a given time period. The length of sampling is selected such that the sampled record includes at least a few full periods (see Fig. 1 for illustration and Fig. 4 for a real measurement). Both receivers (C and D) measure the period length L and the time difference l between the start command and a reference point in the measured signal (in our implementation we use the maximums of the RSSI signal for reference points). The results are sent to the base station where the actual phase difference (offset) is calculated as follows:

$$\vartheta = 2\pi\left(\frac{l_C}{L_C} - \frac{l_D}{L_D}\right)\ (mod\ 2\pi) \tag{3}$$

B. Tracking in one dimension

For tracking in one dimension two fixed transmitter nodes (A and B) and one fixed receiver node C is used, while the tracked receiver is denoted by D (see Fig. 1). The transmitters utilize a single carrier frequency (as opposed to multiple frequencies in [7]) and the receivers continuously monitor the phase difference ϑ. The quad-range d_{ABCD} is calculated. According to (2), the solutions for the position of moving node D are located on a set of hyperboloids (hyperbolas in 2D, as illustrated in Fig. 2). When a ϑ value is measured, the associated quad-range d_{ABCD} determines the possible positions of D. In Fig. 2(a) for illustration purposes hyperbolas corresponding to $2k\pi$ phase values are shown. Note that from one measurement there is no way to determine on which of the possible hyperboloids D is located (i.e. k is unknown), and even if the particular hyperboloid was knew, it is impossible to tell where on the hyperboloid D is exactly located.

We assume that the original location of D is known. Also assuming that the motion of the object is relatively slow, i.e. the successive phase measurements have a difference smaller than π then the actual hyperboloid can be selected, based on the *expected continuity* assumption, using the estimated hyperboloid at the previous time instant, as follows. If the known phase in time instant k is φ_k and the measurement in time instant $k+1$ results the ambiguous phase values $\varphi_{k+1}(i) = \vartheta_{k+1} + 2\pi i$, then the closest possible value to φ_k is selected:

$$i = argmin\ |\vartheta_{k+1} + 2\pi i - \varphi_k| \tag{4}$$

Note that the underlying problem here is in fact the well-known phase-unwrapping problem (see e.g. [8]). In Fig. 2(b) the phase measurements are shown in the range of $(0 \ldots 2\pi)$, while Fig.2(c) shows the phase correction values, according to (4), resulting the unwrapped phase measurement in Fig. 2(d).

Knowing the exact phase value, the actual hyperboloid surface can be identified, using (1) and (2). Thus with a series of measurements the hyperboloid surface on which moving node D is located can be tracked. However, the exact location of D on the hyperboloid is not known yet: for this purpose multiple independent quad-ranges will be used.

C. Tracking in higher dimensions

If in addition to node triplet A,B,C another node triplet A',B',C' is used then two quad-ranges d_{ABCD} and $d_{A'B'C'D}$ can be measured, as shown in Figs. 2(a) and 2(e). Note that node triples A, B, C and A', B', C' may be composed of physically different nodes or alternatively may contain the same nodes but in different roles: e.g. a possible solution is A'=A, B'=C, C'=B.

Using two quad-ranges, two independent one-dimensional tracking can be simultaneously performed, as described in Section III.B. In each time instant each tracking identifies a hyperboloid surface on which node D is located. In Fig. 2 the left and right columns represent the two independent trackings.

Naturally node D is located in the intersection of the two hyperboloids, thus in 2D, the node's location can be calculated, as illustrated in Fig. 2(i). For 3D localization three independent quad-ranges are necessary, for which at least four fixed devices must be used, out of which three independent triplets can be chosen.

The measurements are scheduled using TDMA: different time slices are allocated for each quad-range. In each time-slice two transmitters are transmitting and generate the interference signal at the receivers.

The robustness of the method can be increased by using more quad-ranges: the over-determined system is resistant to bad or missing measurement values. This paper will not cover this topic.

IV. Evaluation

In this section the proposed concept will be evaluated. First the test hardware will be introduced, then phase measurements will be presented to illustrate the feasibility of the proposed approach. Finally a proof-of-concept tracking test will be introduced with four fixed and one moving device.

A. Test hardware

In the tests a special dual-radio node was used, the photo of which is shown in Fig. 3. The nodes are based on Atmel's ATmega128RFA1 microcontroller which operates at 16 MHz and has an on-chip 2.4GHz RF transceiver, providing a cost efficient and integrated solution. This radio is used to transmit start commands and measurement results.

Our node also has another radio chip (Silicon Labs, Si4432) with a wide variety of configuration options. This includes not only the transmission power and frequency band (240-480MHz, 480-930MHz) selection, but the ability of fine tuning the transmission frequency in 156.25 Hz or 312.5 Hz increments. This feature makes the chip suitable for radio interference based tracking where the two transmitted sine waves need to be tuned nearly to the same frequency. In our system this radio is used to perform the interferometric measurements only.

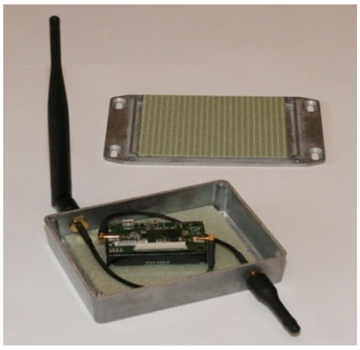

Figure 3. The dual-radio node used in the tests

In our measurements we used the 868MHz ISM frequency band and fine tuned the frequency of one transmitter of each pair. Because the transmitted frequency highly depends on the environmental temperature, the calibration should be done before the actual phase measurement process and it should be corrected if the measured frequency changed too much. The actual RSSI measurement is done by reading the corresponding register from the radio chip in every 1/62500 second 390 times. This data is stored in a memory buffer for frequency and phase estimation, described in Section III.A. In most cases the used frequency difference is set to around 700 Hz, which provides around 90 samples per period. This amount of sample allows accurate phase estimation.

B. *Phase measurements*

To illustrate the phase measurement process, raw RSSI measurement results were downloaded from two synchronized receiver nodes, as shown in Fig. 4. Note that the RSSI output of the radio is logarithmic, that is why the shown envelop has not sinusoidal shape. The carrier frequency of the radios was set to the 868MHz and one of the radios was tuned off by 5937.5Hz. Due to the inaccuracies of the radio devices, this frequency offset resulted approx. 620Hz frequency difference between the two radios. In Fig. 4 the frequency of the measured RSSI signals correspond to this value. The phase difference between the two RSSI signals was $\vartheta = 0.92\pi$, as can be seen in Fig. 4.

The next test was carried out to illustrate the accuracy of the phase offset measurements. Fig. 5 shows the test setup with two fixed transmitters A and B, a fixed receiver C, and a moving node D, which moved along trajectories T1, T2, and T3. The tests were performed outdoors in an orchard where the nodes were placed 1.2m above ground level on a wooden table. Phase offset values were measured along the trajectories in 0.02m increments, collecting 100 measurements in each position. During the measurements the effect of external disturbances was minimized (e.g. there were no movements or operating electronic devices nearby).

The results for trajectories T1, T2, and T3 are shown in Figs. 6, 7, and 8, respectively. The figures show both the wrapped and unwrapped phase offset values. Blue lines denote the computed ideal phase offset, while red dots show the actual measured values. Note the significant variance in the phase offset measurements, despite of the relatively disturbance-free environment. Also note that the variance is safely below the limit of π, thus phase unwrapping is indeed possible using the expected continuity assumption.

The frequency difference Δf varied between 892Hz and 1420Hz during measurement T1, between 3472Hz and 3906Hz during T2, and between 416Hz and 1136Hz during T3. The variance of the phase measurement was the largest in T2, due to the large Δf. Note that the transmission frequency is sensitive to temperature, thus Δf changed quite rapidly during the measurements.

The measurements also show significant local distortions of the phase offset pattern: at certain locations the phase offset values systematically tend to deviate from the ideal values, see e.g. Fig. 6 around position 0.8m or Fig. 8 around 1m. These errors naturally will cause error in the tracking process as well, but are local and do not accumulate.

The distribution of the phase offset was tested with static nodes with frequency difference $\Delta f = 595$Hz-744Hz during the test. Fig. 9(a) shows the disturbance free case, while Fig. 9(b) illustrates the situation when people were moving around the sensors, using 1500 measurements in each case. The standard deviation in the disturbance-free case was 0.03π, which increased to 0.09π when people were present in the measurement space. Fig. 9 shows that in both cases the noise level is small enough to perform phase unwrapping, but when disturbance is present, the phase error between two consecutive measurements may be close to π, thus in this case probably more sophisticated unwrapping techniques should be used.

C. *Object tracking*

A proof of concept test was made to check the tracking capabilities of the proposed method. The test was carried out outdoors, using four fixed nodes and one moving node. The setup is shown in Fig. 10. The fixed nodes had alternating roles: in odd time slices node A and B were transmitting and node A' was receiving; in even time slices node A' and B' were transmitting and node A was receiving (the moving node was receiving in every time slice). The moving node was carried in hand by a person, who walked along the rectangular trajectory, shown by red color in Fig. 10. The walker approached the rectangular path from the north (see the small initial curve at the top of figure) and made three rounds. The

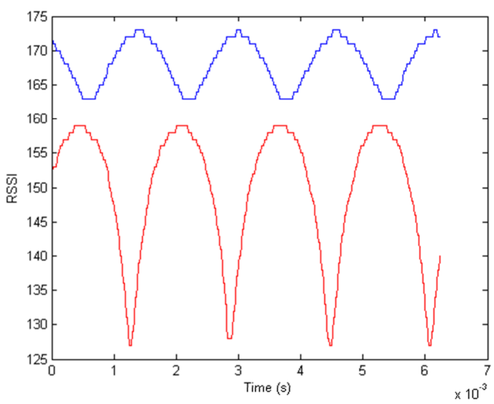

Figure 4. RSSI measurements of an interferometric signal with two synchronized radio receivers (blue and red lines, respectively). The RSSI output of the radio has logarithmic scale.

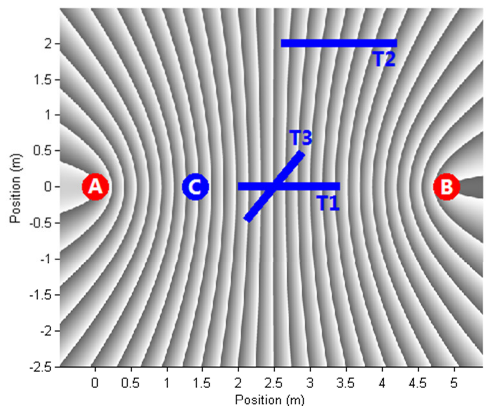

Figure 5. Setup for phase-offset test measurements using fixed transmitters A,B, fixed receiver C, and moving receiver D. Blue line segments show trajectories T1, T2, and T3 of the moving object D. The calculated ideal phase-offset pattern is also shown.

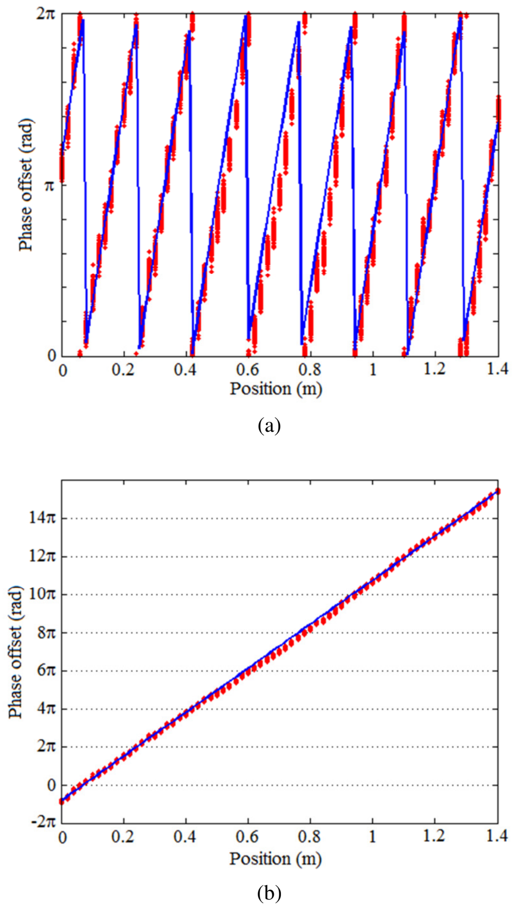

Figure 6. Phase offset measurements for trajectory T1. Blue lines show the ideal phase offset values, scattered plot with red dots show the actual measurements. (a) wrapped and (b) unwrapped phase offset values.

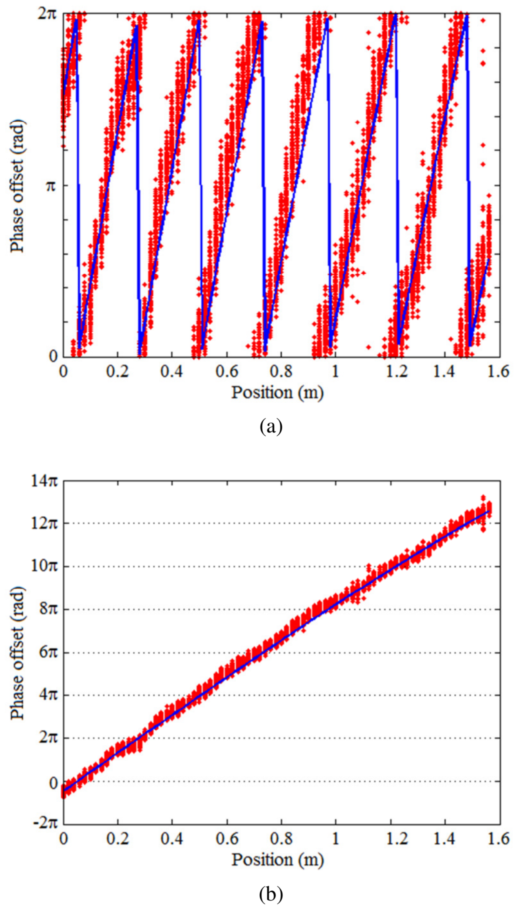

Figure 7. Phase offset measurements for trajectory T2. Blue lines show the ideal phase offset values, scattered plot with red dots show the actual measurements. (a) wrapped and (b) unwrapped phase offset values.

estimated positions are show in Fig. 10 by blue dots.

During the measurement the 868MHz frequency channel was used and the radios were fine tuned to provide $\Delta f_{AB} = 718Hz$ and $\Delta f_{A'B'} = 961Hz$ frequency difference for transmitter pairs (A,B) and (A',B'), respectively. The measurements were scheduled to provide 7 position estimations in each second. Note that each raw phase measurement was used in a new position estimation, there was no preprocessing (averaging or other filtering of phase data) applied. Note that the system can provides real time tracking as opposed to the several minutes long measurement and computing time of [7].

As shown in Fig. 10, the tracking results are promising. The inaccuracies probably originate from two possible sources: (1) the object, carried by a person, did not follow exactly the ideal trajectory, and (2) the phase pattern was probably distorted, especially on the east side of the trajectory. Since the exact trajectory is not known the accuracy cannot be exactly determined, either. The achievable accuracy of the tracking solution is around half of the utilized wavelength (approximately 0.16m in our system), which correlates well with the results shown in Fig. 10.

The accuracy and robustness of the method can probably be increased if redundancy is added to the system. Redundancy can be used either in the computation level (e.g. filtered phase estimates can be used in phase unwrapping process), or more quad-ranges can be used. In the latter case an over-determined equation system has to be solved, where erroneous measurements can be identified and neglected.

V. Conclusion

A novel RF object tracking method was proposed which is able to perform the tracking of objects equipped by a simple radio transceiver, by using repeated phase measurements of interference signals, generated by fixed infrastructure radio transmitters. The radio interference is generated by pairs of transmitters and phase offset is measured between the moving node and a fixed infrastructure receiver.

The feasibility of the proposed method was illustrated by real measurements and preliminary experiments. The accuracy of the phase measurement and a simple unwrapping technique was illustrated, and a four-node 2D tracking experiment was also discussed.

The first outdoor experiments are promising, however the applicability of the proposed approach in indoor environments,

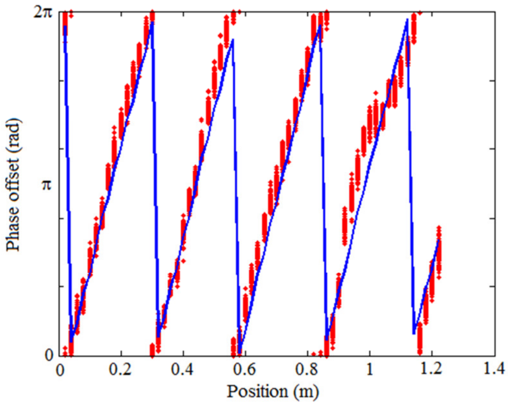

(a)

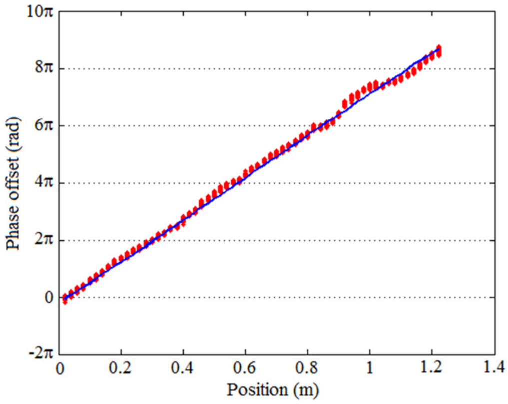

(b)

Figure 8. Phase offset measurements for trajectory T3. Blue lines show the ideal phase offset values, scattered plot with red dots show the actual measurements. (a) wrapped and (b) unwrapped phase offset values.

where fading is a critical issue, is to be further examined. By adding redundancy to the system its robustness can be increased, thus errors from signal loss can be eliminated. Also more advanced unwrapping techniques, using built-in models on the movement, can be applied to increase the robustness of the system.

References

[1] T Ajdler, I. Kozintsev, R. Lienhart, M. Vetterli, "Acoustic source localization in distributed sensor networks," Conference Record of the Thirty-Eighth Asilomar Conference on Signals, Systems and Computers, 2004, vol.2, pp.1328-1332, Nov. 2004

[2] A. Mulloni, D. Wagner, I. Barakonyi, D. Schmalstieg, "Indoor Positioning and Navigation with Camera Phones," IEEE Pervasive Computing, vol. 8, no. 2, pp. 22-31, April-June, 2009

[3] Kai Ni; A. Kannan, A. Criminisi, J. Winn, "Epitomic location recognition," IEEE Conference on Computer Vision and Pattern Recognition, CVPR 2008., pp.1-8, June 2008

[4] Anthea Wain Sy Au et al, "Indoor Tracking and Navigation Using Received Signal Strength and Compressive Sensing on a Mobile Device," IEEE Transactions on Mobile Computing. IEEE computer Society Digital Library. IEEE Computer Society, pp. 2050-2062, Aug. 2012

[5] S. Lanzisera, D.T. Lin, K.S.J. Pister, "RF Time of Flight Ranging for Wireless Sensor Network Localization," 2006 International Workshop on Intelligent Solutions in Embedded Systems, pp.1-12, June 2006

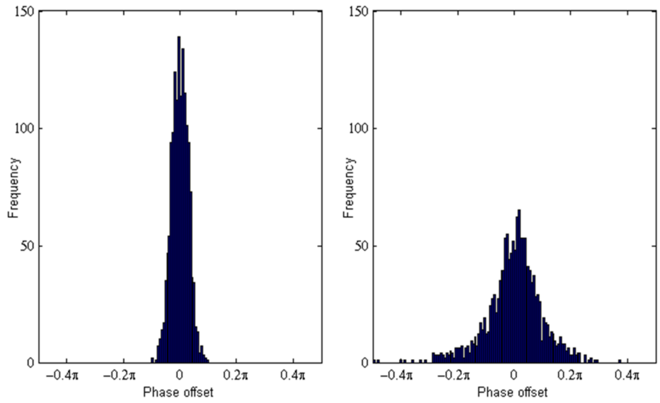

(a) (b)

Figure 9. Distribution of 1500 phase offset measurements (a) disturbance-free case (b) human presence and movement

[6] S. Schwarzer, M. Vossiek, M. Pichler, A. Stelzer, "Precise distance measurement with IEEE 802.15.4 (ZigBee) devices," 2008 IEEE Radio and Wireless Symposium, pp.779-782, Jan. 2008

[7] M. Maroti et al, "Radio Interferometric Geolocation", ACM Third International Conference on Embedded Networked Sensor Systems (SenSys 05), San Diego, CA, pp. 1--12, November, 2005.

[8] J.M. Tribolet, "A new phase unwrapping algorithm", IEEE Transactions on Acoustics, Speech, and Signal Processing, ASSP, Vol. 25, No.2, pp. 170-177, Apr. 1977.

[9] J. Elson, L. Girod, and D. Estrin, "Fine-grained network time synchronization using reference broadcasts". *SIGOPS Oper. Syst. Rev.* Vol. 36, No. SI, pp. 147-163, Dec. 2002.

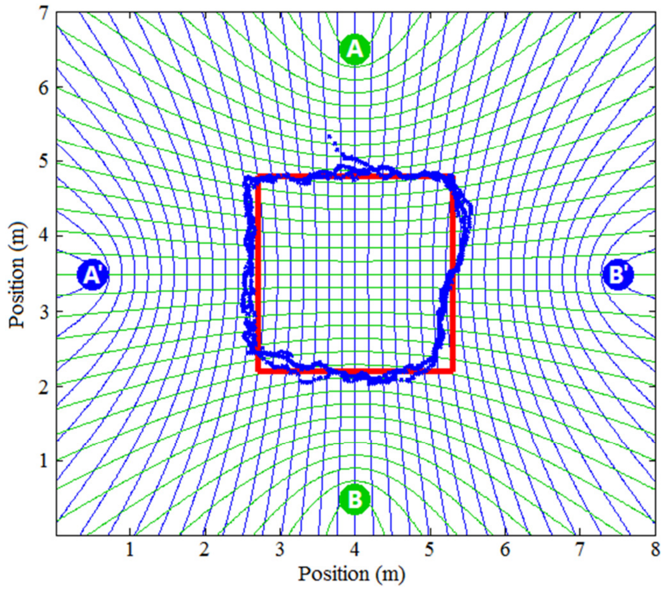

Figure 10. Radiointerferometric tracking. The fixed nodes were nodes A,B,A', and B', with periodically changing roles. The moving object was carried on the rectangular path denoted by the red line. The tracked positions are shown by blue dots. The ideal phase patterns are also shown: green lines for trasmitter pair (A,B), blue lines for transmitter pair (A',B')